Developmental Biology 430 (2017) 69–79

Contents lists available at ScienceDirect

Developmental Biology

journal homepage: www.elsevier.com/locate/developmentalbiology

Loss of zinc finger MYND-type containing 10 (zmynd10) affects cilia integrity and axonemal localization of dynein arms, resulting in ciliary dysmotility, polycystic kidney and scoliosis in medaka (*Oryzias latipes*)

Daisuke Kobayashi[a,*], Anshin Asano-Hoshino[b], Takashi Nakakura[b], Toshiyuki Nishimaki[c], Satoshi Ansai[d,1], Masato Kinoshita[d], Motoyuki Ogawa[c], Haruo Hagiwara[b], Takahiko Yokoyama[a]

[a] Department of Anatomy and Developmental Biology, Graduate School of Medical Science, Kyoto Prefectural University of Medicine, Kyoto, Japan
[b] Department of Anatomy and Cell Biology, Teikyo University School of Medicine, Tokyo, Japan
[c] Department of Anatomy, Kitasato University School of Medicine, Kanagawa, Japan
[d] Division of Applied Bioscience, Graduate School of Agriculture, Kyoto University, Kyoto, Japan

ARTICLE INFO

Keywords:
Cilia
Primary ciliary dyskinesia (PCD)
Polycystic kidney disease (PKD)
Scoliosis
Medaka

ABSTRACT

Cilia and flagella are hair-like organelles that project from the cell surface and play important roles in motility and sensory perception. Motility defects in cilia and flagella lead to primary ciliary dyskinesia (PCD), a rare human disease. Recently *zinc finger MYND-type containing 10* (*ZMYND10*) was identified in humans as a PCD-associated gene. In this study, we use medaka fish as a model to characterize the precise functions of zmynd10. In medaka, *zmynd10* is exclusively expressed in cells with motile cilia. Embryos with *zmynd10* Morpholino knockdown exhibited a left-right (LR) defect associated with loss of motility in Kupffer's vesicle (KV) cilia. This immotility was caused by loss of the outer dynein arms, which is a characteristic ultrastructural phenotype in PCD. In addition, KV cilia in *zmynd10* knockdown embryos had a swollen and wavy morphology. Together, these results suggest that zmynd10 is a multi-functional protein that has independent roles in axonemal localization of dynein arms and in formation and/or maintenance of cilia. The C-terminal region of zmynd10 has a MYND-type zinc finger domain (zf-MYND) that is important for its function. Our rescue experiment showed that the zmynd10−ΔC truncated protein, which lacks zf-MYND, was still partially functional, suggesting that zmynd10 has another functional domain besides zf-MYND. To analyze the later stages of development, we generated a *zmynd10* knockout mutant using transcription activator-like effector nuclease (TALEN) technology. Adult mutants exhibited sperm dysmotility, scoliosis and progressive polycystic kidney.

1. Introduction

Cilia are evolutionarily ancient organelles whose structure and function have been highly conserved among species, from unicellular organisms to higher vertebrates. Cilia are hair-like organelles that project from the cell surface and have many functions. Disruption of one or more of these functions leads to a diverse set of human diseases, collectively known as ciliopathies. There are two types of cilia: immotile and motile cilia/flagella. Among the ciliopathies, a motility defect involving the cilia and flagella is referred to as primary ciliary dyskinesia (PCD), and is characterized by recurrent respiratory tract infections, sinusitis, bronchiectasis, male infertility and randomization of left-right (LR) body asymmetry. More than 30 genes have been identified as causal genes in PCD (OMIM; CILIARY DYSKINESIA, PRIMARY CILD; (Kurkowiak et al., 2015; Kobayashi and Takeda, 2012).

Most motile cilia/flagella are composed of nine peripheral outer doublet microtubules (MT), surrounding a central pair of microtubule apparatus (CP, a 9 + 2 arrangement). In contrast, in nodes and Kupffer's vesicles (fish organs that are functionally equivalent to the mouse node in terms of LR specification), cilia lack CP (that is, a 9 + 0 arrangement). Several accessory structures are associated with the MT pairs, including radial spokes, nexin links (a dynein regulatory complex) and outer or inner dynein arms (ODAs or IDAs). Disruption of these structures is associated with the development of PCD (Kobayashi

* Corresponding author.
E-mail addresses: kdaisuke@koto.kpu-m.ac.jp (D. Kobayashi), anshin@med.teikyo-u.ac.jp (A. Asano-Hoshino), nakakura@med.teikyo-u.ac.jp (T. Nakakura), nmaki@med.kitasato-u.ac.jp (T. Nishimaki), ansai@nig.ac.jp (S. Ansai), kinoshit@kais.kyoto-u.ac.jp (M. Kinoshita), ogwmedu@kitasato-u.ac.jp (M. Ogawa), hhagiwar@med.teikyo-u.ac.jp (H. Hagiwara), tyoko@koto.kpu-m.ac.jp (T. Yokoyama).
[1] Present addresse: Division of Ecological Genetics, Department of Population Genetics, National Institute of Genetics, Shizuoka, Japan.

http://dx.doi.org/10.1016/j.ydbio.2017.08.016
Received 23 March 2017; Received in revised form 10 August 2017; Accepted 10 August 2017
Available online 16 August 2017

and Takeda, 2012).

In fish embryos, epithelial cells with motile cilia are highly abundant in Kupffer's vesicle (KV), the otic vesicle and the pronephric tubule (previously called the pronephric duct). Motile cilia in these structures are important for LR body axis determination, otolith formation and urine excretion, respectively (Riley et al., 1997; Kramer-Zucker et al., 2005; Essner et al., 2002). In zebrafish embryos, motile ciliary genes are abundantly expressed in highly ciliated tissues, and these genes are regulated by foxj1 transcription factors (Yu et al., 2008; Stubbs et al., 2008). These genes, being expressed in similar complex patterns, are said to belong to a “synexpression” group. Such groups often encode proteins that function in a common pathway (Gawantka et al., 1998; Kudoh et al., 2001).

Initially identified as a candidate functional tumor suppressor gene (Lerman and Minna, 2000), *zinc finger MYND-type containing 10* (*zmynd10*) is one of a group of genes that were detected as abundantly expressed in tissues that are rich in ciliated cells (McClintock et al., 2008). It was also observed that *zmynd10* was more than 4-fold up-regulated in multi-ciliated tracheal epithelial cells when ciliogenesis was induced (Hoh et al., 2012). Albee *et al.* reported that the *Chlamydomonas* homolog, *Cre08.g358750*, was up-regulated almost 29-fold during ciliogenesis (Albee et al., 2013). Moreover, knockdown of *ZMYND10* in hTERT-RPE1 cells affected ciliary length and basal body/centriole number. Recently *ZMYND10* was identified as a causal gene for PCD in humans (Moore et al., 2013; Zariwala et al., 2013), and both ODAs and IDAs are absent in cilia isolated from affected individuals. Such morphological phenotypes are characteristic of cytoplasmic dynein arm assembly defects. They also showed that ZMYND10 interacts with LRRC6 (Leucine Rich Repeat Containing 6), another cytoplasmic factor required for dynein arm assembly. Together, these results suggest that ZMYND10 functions in cytoplasmic dynein arm assembly.

Idiopathic scoliosis (IS) is characterized by abnormal lateral curvature of the spine. An integrative model of the etiopathogenesis of IS has been proposed, with genetic factors thought to be among the underlying causes of IS (Wang et al., 2011). Recently, a study of zebrafish with mutations in motile cilia-related genes led to the suggestion that there might be a link between IS and cerebrospinal fluid (CSF) flow (Grimes et al., 2016). Our group and that of Nagao et al. (2010), also reported motile ciliary mutants with scoliosis (note that in our original paper the phenotype was represented as a severely wavy trunk or axial structural abnormalities, but these features are hereafter referred to as ′scoliosis′), and proposed that scoliosis might be related to CSF flow (Kobayashi et al., 2010). The common phenotype of these fish mutants suggested that motile ciliary defects might be one of the underlying causes of scoliosis.

Here, we report that reduced zmynd10 activity in medaka (*Oryzias latipes*) leads to ODA loss in KV cilia, and results in a motility defect. Morphants had curly-tail-down (CTD) and LR randomization, which are characteristic motile ciliary mutant phenotypes in fish. Ultrastructural analyses of morphants showed that zmynd10 is required both for correct axonemal localization of dynein arms and for formation and/or maintenance of cilia. Furthermore, in *zmynd10* knockout (KO) medaka analyzed at later stages of development, there was complete loss of sperm motility, scoliosis and progressive polycystic kidney.

2. Materials and methods

2.1. Fish strains

All experiments were approved by the ethics committee of Kyoto Prefectural University of Medicine (KPUM). Fish were maintained in a constant re-circulating system in the central animal facility of KPUM at 28 °C on a 14-h light/10-h dark cycle. The d-rR medaka strain was obtained from the medaka National BioResource Project (NBRP; Okazaki, Japan). Embryos were staged according to the Iwamatsu protocol (Iwamatsu, 2004).

2.2. Whole mount in situ hybridization, immunohistochemistry and histology

Whole mount in situ hybridization (WISH), immunohistochemistry (IHC) and histological analysis were performed as described previously (Nagata et al., 2016; Takashima et al., 2007). The stained embryos were cut into 30-μm sections using a cryostat.

2.3. Morpholino knockdown, mRNA injection and determination of LR laterality

Antisense Morpholinos (Mos) directed against the medaka *zmynd10* mRNA translation initiation site and exon 1 splice donor site were 5′-ATACCAGTCGTTTCCATTTTGTGTC-3′ (TB) and 5′-CGTTTGTTTATATCTTCTTACCTTA-3′ (SB), respectively (Fig. S1; Gene Tools, OR, USA). Five-base mismatch Mos against *zmynd10*, 5′-ATACgAcTCcTTTCgATTTTcTGTC-3′ (TB-5mis) and 5′-CGTTaGaTTATATgTTgTTAgCTTA-3′ (SB-5mis) were used as a negative control (mismatch nucleotides are indicated in lower case). The Mo directed against the medaka dynein axonemal intermediate 2a (dnai2a) exon 1 splice donor site was 5′-TTAACTGTGACTTGTCTTGCCTCGT-3′ (Mo-dnai2a-E1I1). The Mos were dissolved in Yamamoto's Ringer solution. For mRNA synthesis, *zmynd10* cDNA was cloned into the pCS2+ plasmid vector. Plasmids were linearized and mRNA synthesized using a mMESSAGE mMACHINE SP6 kit (Ambion, TX, USA), after which the mRNA was diluted with Yamamoto's Ringer solution prior to injection.

Organ laterality was determined at stage 34, when both cardiac looping and the liver position are easily observable. Embryos with reversed heart looping and/or reversed positioning of the liver were classified as having an LR defect (Fig. S2).

2.4. The transcription activator-like effector nuclease (TALEN) design and synthesis

TALEN reagents used in this study were designed and constructed according to the protocol of Ansai et al. (2013). Briefly, we searched TALEN targeting sequences using TALEN Targeter (https://boglab.plp.iastate.edu/node/add/talen) and selected exon 2 of the medaka *zmynd10* gene. Repeat-variable di-residue (RVD) sequences in the TAL Effector DNA-binding domains were NN-NN-NG-NG-HD-NI-HD-NI-HD-NI-NI-HD-NI-HD-NN-NI for the left arm and HD-HD-NI-NN-HD-NI-HD-NG-NN-HD-HD-NG-NN-HD-NI-NG-NN-NG for the right arm.

2.5. Cilia observations

Embryos were fixed and processed as described previously (Omran et al., 2008), and whole KV cilia movement was captured using a BZ-9000 fluorescence microscope (KEYENCE, Osaka, Japan) according to the protocol of Kamura et al. (2011). Sperm motility was captured using an Olympus BX51 microscope fitted with a 40× lens (OLYMPUS, Tokyo, Japan) and an ORCA_Flash4.0 digital camera (HAMAMATSU, Hamamatsu, Japan). Movies were acquired at approximately 200 frames per second (fps) and played at 25 fps.

3. Results

3.1. zmynd10 is a MYND-type zinc finger containing protein

We hypothesized that a synexpression group that is commonly expressed in motile ciliated tissues could be used to identify motile cilia-related and PCD candidate genes. We searched the zebrafish expression database (http://zfin.org/) for genes commonly expressed

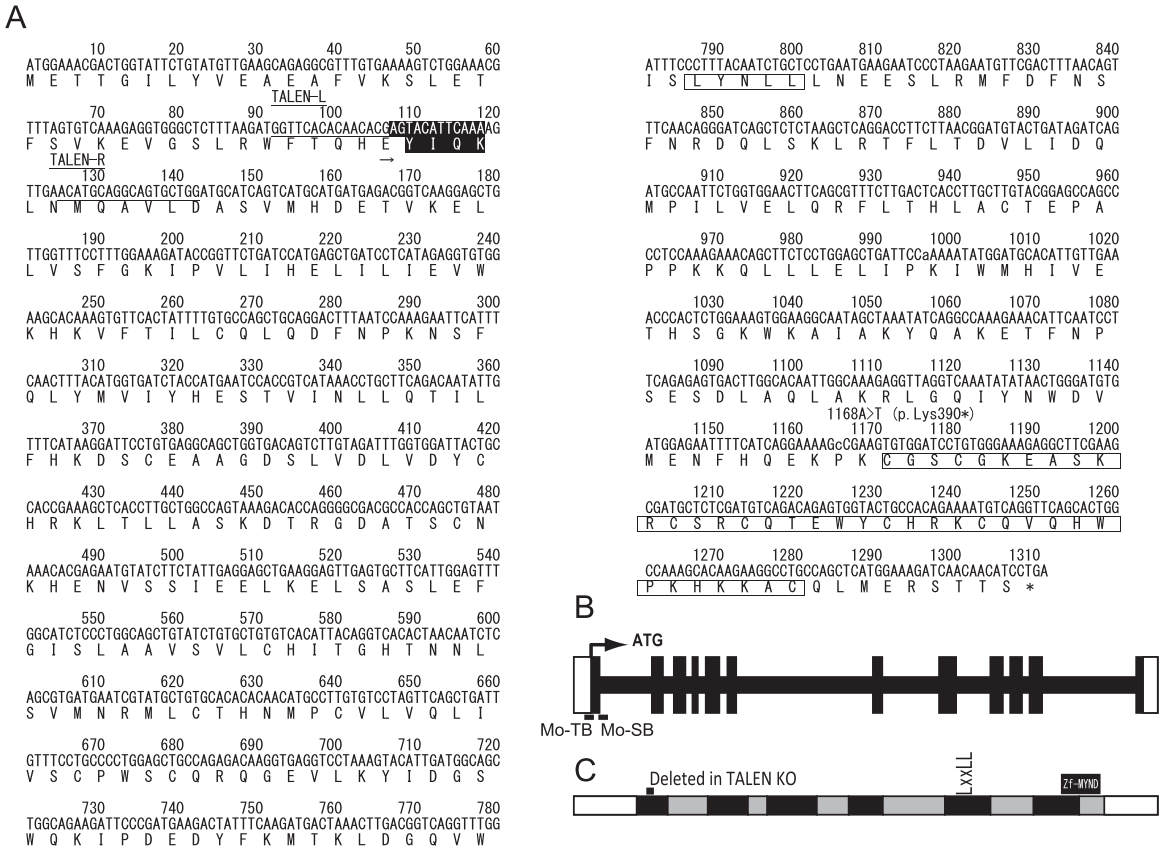

Fig. 1. Medaka zinc finger MYND-type containing 10 (zmynd10). (A) Medaka zmynd10 orf and deduced amino acid sequence. Transcription activator-like effector nuclease (TALEN) target sites are underlined. The deleted sequence in the mutant is shown in white characters and the conserved LxxLL and zf-MYND motifs are boxed. (B) Exon/intron structure of medaka *zmynd10*. Exons are represented by vertical bars (coding regions are indicated by dark fill) and introns are represented by the horizontal regions in between. The positions of the start codon (ATG) and Morpholino target sites are indicated (MO-TB and MO-SB). (C) Domain structure of medaka zmynd10. The conserved LxxLL motif, zf-MYND domain and the deleted sequence in the TALEN KO fish are indicated.

in KV, the otic vesicle and the pronephric tubule, and identified *zmynd10* (previously named zgc:63660). Several bioinformatic analyses have suggested that *zmynd10* is a ciliary gene, even though they did not identify *zmynd10* as a motile cilia-specific gene (McClintock et al., 2008; Ross et al., 2007). Moreover, it has been reported that the ZMYND10 gene is causal for PCD (Moore et al., 2013; Zariwala et al., 2013), suggesting that zmynd10 may be indispensable for motile cilia.

Medaka *zmynd10* cDNA was cloned from kidney cells and sequenced. Medaka *zmynd10* encodes a 436-aa protein (DDBJ entry ID, 58d0b4242113a518e5004d1d), and a search of the Pfam database (http://pfam.xfam.org/) predicts only the presence of a MYND-type zinc-finger domain (zf-MYND) at its C-terminal region (boxed in Fig. 1A; Fig. S3). Sequence similarity between vertebrates and *Drosophila* was not restricted to the zf-MYND domain, but was found throughout the sequence (Fig. S3). Only one of the four LxxLL motifs predicted in humans was conserved in medaka (boxed in Fig. S3).

3.2. *zmynd10 is expressed in tissues with motile cilia*

Because *zmynd10* is selectively expressed in zebrafish tissues with motile cilia, we proposed that *zmynd10* is a motile cilia-related gene. First, we assessed if *zmynd10* expression is conserved in medaka. As expected, *zmynd10* RNA expression was detected in tissues with motile cilia, including KV (stage 18 in Fig. 2A, F), the pronephric tubules (stages 24 and 31 in brackets in Fig. 2B, C) and the otic vesicle (stage 31 indicated by arrowhead in Fig. 2D). Transverse sections showed that *zmynd10* is expressed in the pronephric tubule (stages 24 and 31; indicated by arrowheads and dashed circle in Fig. 2H and I, respectively). In KV, *zmynd10* expression was already detectable in stage 17 embryos (Fig. 2E), and expression persisted to stage 22 (Fig. 2G). Combined, our results show that *zmynd10* is expressed in medaka tissues with motile cilia in a similar manner to that reported in zebrafish (http://zfin.org/), mouse and *Drosophila* (Moore et al., 2013).

3.3. *zmynd10 is required for LR specification*

To elucidate the function of *zmynd10*, we injected a translation-blocking (TB) and/or a splice-blocking (SP) Mo into wild-type (WT) embryos at the single-cell stage (Mo-TB and Mo-SP in Fig. 1B and Fig. S1). Mo-injected embryos (morphants) presented with LR defects in a dose-dependent manner (Fig. 3; Table 1; Fig. S2), and co-administration of Mo-TB and Mo-SP synergistically affected LR determination. The LR defect phenotype varied between morphants (Fig S2). Embryos with reversed (Fig. S2 Ba, Da) or ambiguous heart looping (midline heart loops in Fig S2 Ea,) and/or reversed liver position (Fig. S3 Bb, Cb) were classified as having an LR defect. When greater than 100 μM of each Mo was injected, approximately half of the morphants had LR inversion of their internal organs (LR randomization), whereas simultaneous administration of Mo-TB-5mis and Mo-SB-5mis resulted in a very low frequency of this abnormality (Table 1). To provide further evidence that *zmynd10* is required for correct LR development, we rescued the LR defect by injecting mRNA encoding the complete WT *zmynd10* coding sequence into *zmydn10* morphants. WT *zmynd10* mRNA expression completely corrected the LR defect of the morphants (Table 1). To examine whether there is functional conservation among species, we cloned mouse *Zmynd10* and found that Zmynd10 partially rescued medaka *zmynd10* morphants (Table 1). This result suggests that zmynd10 function is conserved among species. Taken together,

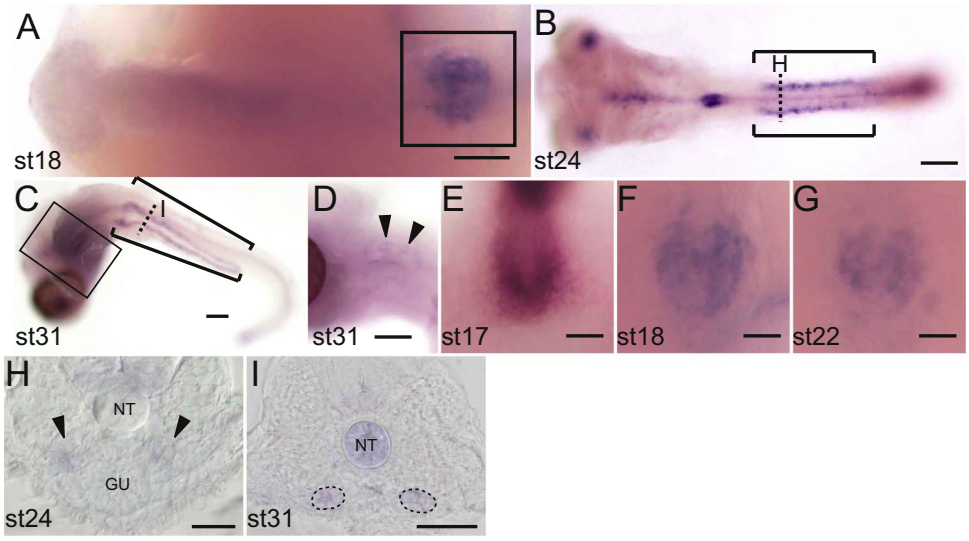

Fig. 2. Gene expression pattern of *zmynd10* in medaka embryos. (A) *zmynd10* expression in Kupffer's vesicles (KV) at stage 18. The box indicates the region enlarged in F. (B, C) *zmynd10* expression in the pronephric system at stage 24 (B, brackets) and stage 31 (C, brackets). The dashed lines represent the approximate levels of the transverse sections shown in H and I, respectively. The box in C indicates the region enlarged in D. (D) *zmynd10* expression in the otic vesicles (arrowheads). (E–G) Dorsal views of stages 17 (E), 18 (F) and 22 (G). By stage 17, *zmynd10* expression is evident in KVs and persists to stage 22. (H, I) *zmynd10* expression in transverse sections of the pronephric tubule at stages 24 (H, arrowheads) and 31 (I, dashed circles). NT, notochord; GU, gut. Scale bars: A–G, 100 μm; H and I, 20 μm.

these experiments provide convincing evidence that zmynd10 is required for LR axis formation.

To molecularly characterize the LR phenotype of the *zmynd10* morphants, we analyzed the localization of *southpaw* (*spaw*) and *charon* in *zmynd10* morphants. *Spaw*, which is normally expressed in the left lateral-plate mesoderm (LPM; nine-somite stage in Fig. 3Ba), was diffusely expressed, with reduced or absent expression in both sides of the LPM and reversed laterality (total sample size, n = 25; normal left side position, n = 9; bilateral position, n = 12; reduced or absent expression, n = 1; right position, n = 3; Fig. 3Bc–f; Fig. S4) (Hojo et al., 2007; Long et al., 2003). In the control morphants *spaw* was expressed in the left side of the LPM (n = 5; Fig. 3Bb; Fig. S4). *Charon* is the earliest LR gene to show asymmetric expression in KV (Fig. 3Ca) (Hojo et al., 2007). Its right-biased asymmetrical expression,

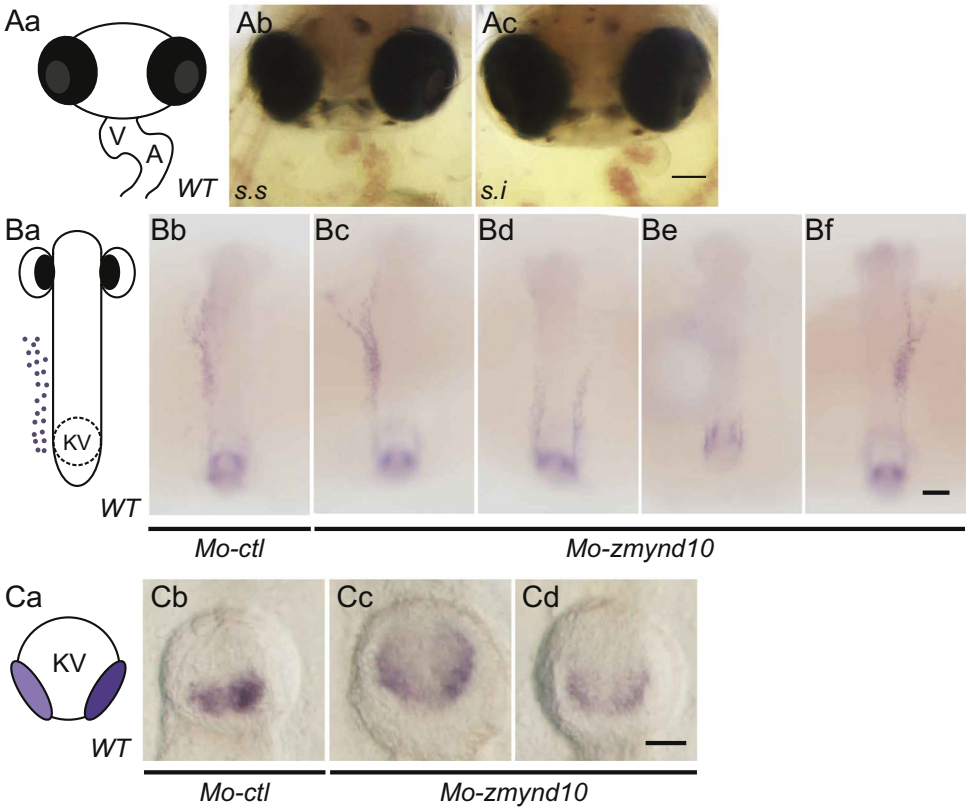

Fig. 3. Medaka *zmynd10* morphant embryos showing L-R randomization. (A) Heart looping at stage 35 in the wild-type (WT) medaka (schematic diagram in Aa; A, atrium; V, ventricle), the control morphant (Ab) and the *zmynd10* morphant (Ac). (B) *Spaw* expression in the WT medaka (schematic diagram in Ba; purple dots represent *spaw* expression), the control morphant (Bb) and the *zmynd10* morphant (Bc–Bf) at the nine-somite stage. (C) *Charon* expression in the WT (Ca, schematic diagram), the control morphant (Cb) and the *zmynd10* morphant (Cc, Cd) at the eight-somite stage. Scale bars: A and B, 100 μm; C, 50 μm.

Table 1
Morpholino injection with or without mRNAs.

Mo-*zmynd10* (μM)		mRNA (ng/μL)	LR-defect		Counted		Total
Mo-TB	Mo-SB	*zmynd10*	#	%	#	%	
200	0	0	0	0.0	13	52.0	25
400	0	0	5	18.5	27	54.0	50
600	0	0	17	47.2	36	55.4	65
800	0	0	46	47.9	96	68.6	140
0	200	0	0	0.0	12	70.6	17
0	400	0	2	5.0	40	61.5	65
0	600	0	6	15.0	40	62.5	64
0	800	0	14	34.1	41	46.1	89
6.25	6.25	0	3	3.5	86	72.3	119
12.5	12.5	0	14	25.9	54	72.0	75
25	25	0	28	50.9	55	73.3	75
50	50	0	30	63.8	47	62.7	75
100	100	0	17	51.5	33	66.0	50
200	200	0	48	68.6	70	56.0	125
400	400	0	15	62.5	24	48.0	50
200 (5mis)[a]	200 (5mis)[a]	0	2	2.9	68	57.1	119
200	200	250 (medaka WT)	0	0.0	45	60.0	75
200	200	250 (mouse WT)	11	16.2	68	56.7	120
200	200	488 (mouse WT)	11	16.7	66	69.5	95

Total: The total number of injected embryos.
Counted: The remaining number of embryos after deduction of those for which laterality could not be determined (dead or abnormal development).
% of Counted: (Counted / Total) × 100.
% of LR-defect: (LR-defect / Counted) × 100.
[a] Mo-TB-5mis and Mo-SB-5mis, respectively.

which was observed in the eight-somite stage WT embryos, was lost in *zmynd10* morphants (n = 6, Fig. 3Cc and data not shown). Although *charon* expression was symmetrical in the morphants, the expression levels were variable; that is, they were upregulated in some embryos and downregulated in others. In the control morphants, *charon* expression was the same as in WT embryos (n = 6, Fig. 3Cb and data not shown). These results suggest that *zmynd10* acts upstream of *charon*.

3.4. Genetic interaction of zmynd10 and dnai2a in LR development

The events upstream of *charon* that disrupt symmetrical development during early embryogenesis are associated with the establishment of unidirectional flow by motile cilia within KV in the teleost (Essner et al., 2002; Hojo et al., 2007; Brummett and Dumont, 1978). Disruption of this flow can give rise to abnormal LR asymmetry. We investigated whether zmynd10 is involved in the ciliary processes that are associated with LR development. To do this, we combined *zmynd10* and *dnai2a* knockdowns, since *dnai2* is a component of the ODA and *dnai2* mutations cause the ciliary dysmotility that results in LR randomization in humans and medaka (Fig. S5) (Kobayashi et al., 2010; Nagao et al., 2010; Loges et al., 2008). While individual injections of a suboptimal dose of Mos against either *zmynd10* or *dnai2a* showed incomplete LR randomization, simultaneous injections acted in synergy to induce complete LR randomization. This result shows that there is a genetic interaction between *zmynd10* and *dnai2a* (Table 2), and suggests that zmynd10 is involved in ciliary function in KV.

3.5. zmynd10 is required for ciliary motility in KV

We next investigated whether the *zmynd10* knockdown affects KV cilia formation and/or function. Immunolocalization of acetylated-α-tubulin at the nine-somite stage showed no significant differences in KV cilia axonemal structure between the control and the *zmynd10* morphant (Fig. 4A and B). These data suggest that cilia axonemal structure is unaffected in *zmynd10* morphants. We next examined KV ciliary motility and found complete immotility in the *zmynd10* morphants (Video 1, zmynd10 morphant; Video 2, control morphant). These data suggest that loss of KV cilia motility is causative for the LR defect in *zmynd10* morphants.

3.6. zmynd10 is required for ODA localization and normal ciliary shape in KV

We used transmission electron microscopy (TEM) to examine the effect of zmynd10 disruption on the ciliary ultrastructure. Cross-sections of KV cilia showed ODA defects (Fig. 4C and D). Whereas the ODAs were anchored to the doublet A-tubules in WT KV (Fig. 4C), the ODAs were missing in the *zmynd10* morphant (Fig. 4D). This phenotype resembles that observed in cilia from patients with *ZMYND10* mutations (Moore et al., 2013; Zariwala et al., 2013). We concluded that impaired zmynd10 function prevents correct ODA microtubule localization in KV cilia, resulting in a motility defect. In addition to this defect, *zmynd10* morphant cilia appeared to be swollen (Fig. 4D and control in 4 C). To confirm this phenotype, the ciliary shape was assessed using scanning electron microscopy (SEM). The average diameters were 180.7 ± 24.5 nm (n = 97) in *zmyd10* morphants and 170.5 ± 24.7 nm (n = 59) in control morphants ($p < 0.01$; Fig. 4E–G). SEM analysis also revealed that ciliary shape was wavy in the *zmynd10* morphant (Fig. 4F and control in 4E). Together, our results reveal that zmynd10 is required for ODA localization and correct ciliary morphology and/or maintenance.

3.7. C-terminal truncated zmynd10 mRNA partially rescues the LR phenotype

Our results showed that C-terminal zf-MYND was conserved among vertebrates and *Drosophila*; therefore, we examined the importance of zf-MYND using N- or C-terminal truncated proteins (Fig. 5A). Since 250 ng/μL of WT mRNA rescued the *zmynd10* morphant completely (Table 1), we simultaneously injected equimolar amounts of N- or C-terminal truncated mRNA with MoTB and MoSB. Simultaneous injection of an N-terminally HA-tagged zmynd10 C-terminal region encompassing zf-

Table 2
Genetic interaction between *zmynd10* and *dnai2a*.

Mo (μM)			LR-defect		Counted		Total
*zmynd10*_ATG	*zmynd10*_E1I1	*dnai2a*_E1I1	#	%	#	%	
6.25	6.25	0	2	3.9	51	68.0	75
0	0	60	6	13.6	44	58.7	75
6.25	6.25	60	22	56.4	39	52.0	75

Total: The total number of injected embryos.
Counted: The remaining number of embryos after deduction of those for which laterality could not be determined (dead or abnormal development).
% of Counted: (Counted / Total) × 100.
% of LR-defect: (LR-defect / Counted) × 100.

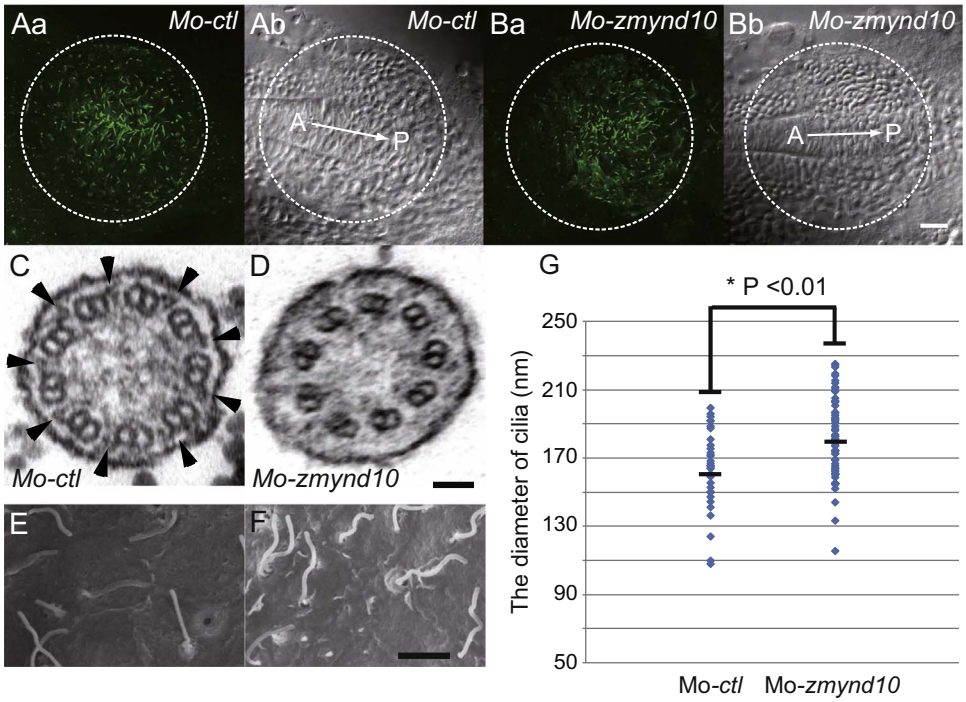

Fig. 4. Cilia phenotype in the *zmynd10* morphant Kupffer's vesicle. Kupffer's vesicle (KV) cilia were detected by anti-acetylated-α-tubulin antibodies (green) in both the control (Aa) and *zmynd10* morphant (Ba). Anterior left ventral differential interference contrast (DIC) images of both the control (Ab) and *zmynd10* morphant (Bb) KVs. KVs are indicated by dashed circles in A and B (A, anterior; P posterior). Transmission electron micrograph of the control (C) and *zmynd10* morphant (D) KV cilia. Outer dynein arms are indicated by arrowheads in C, and are absent in D. Scanning electron micrographs of control (E) and *zmynd10* morphant (F) cilia in KVs. (G) The ciliary diameters of the control and *zmynd10* morphant KVs in E and F. Scale bars: A and B, 20 μm; C and D, 50 nm; E and F, 2 μm.

MYND (Fig. 5A, 391–436 aa, HA+zmynd10–ΔN) did not rescue the *zmynd10* morphant's LR defect, suggesting that zf-MYND alone is insufficient for zmynd10 function. In contrast, zmynd10 lacking the C-terminal region encompassing zf-MYND (Fig. 5A, 1–390 aa, zmynd10–ΔC) partially rescued the LR defect (Fig. 5B).

Since TB-Mo had 17 nucleotides with identity to zmynd10 translation initiation site (Fig. S1), we performed a rescue experiment against *zmynd10* KO fish (described below) to rule out the possibility that the injected mRNA sequestered TB-Mo. A stop codon was introduced by point mutation at c.1168 A > T (p. Lys390*) (Fig. 1; Fig. 5A). To confirm protein expression, we added a 3×FLAG tag sequence at the N-terminus of WT zmynd10 (3 × FLAG-zmynd10-WT) and zmynd10-ΔC (3×FLAG-zmynd10-ΔC; Fig. 5A). When 150 ng/μL 3 × FLAG-zmynd10-WT was introduced into WT embryos it acted in a weak dominant negative fashion (Fig. 5C). When we decreased the 3 × FLAG-zmynd10-WT concentration to 50 ng/μL, this dominant negative effect disappeared. Since 3 × FLAG-zmynd10-ΔC functions in the same way as 3 × FLAG-zmynd10-WT, we also attempted the rescue experiment at 50 ng/μL. Equimolar amounts of membrane-bound green fluorescent protein (gfp-f, 80 ng/μL) was used as a negative control. At this reduced concentration, even 3 × FLAG-zmynd10-WT did not rescue *zmynd10* KO fish completely; therefore, we statistically analyzed the rescue capacity of these constructs. Since the *zmynd10* KO fish are a recessive mutant that shows LR randomization, the probability of the LR defect was set to 12.5% and analyzed using a one-sided binomial test. Our results revealed that both the 3×FLAG-zmynd10-WT and 3 × FLAG-zmynd10- ΔC had statistically-significant rescue effects (Fig. 5C, $P < 0.05$). Together, these results suggest that zmynd10-ΔC retains part of its function.

3.8. *zmynd10 KO fish developed scoliosis, polycystic kidney and sperm immotility*

To study the functions of zmynd10 in the later stages of development, we used TALEN to generate *zmynd10* KO fish (Ansai et al.,

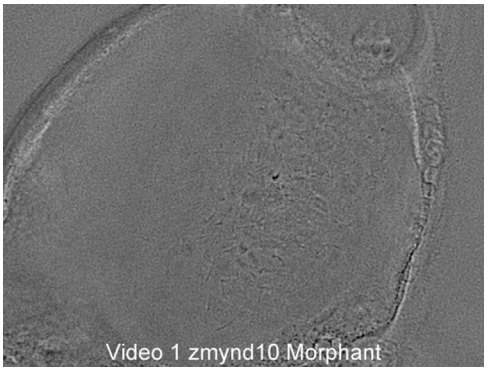

Video 1. Dorsal view of KV cilia in the *zmynd10* morphant showing complete blockage of cilia rotation. Supplementary material related to this article can be found online at http://doi:10.1016/j.ydbio.2017.08.016.

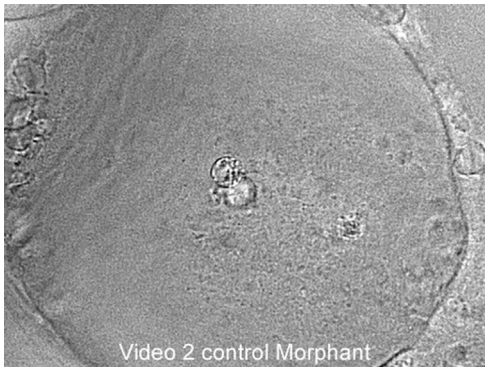

Video 2. Dorsal view of KV cilia in the control morphant showing cilia rotation on KV epithelial cells. Supplementary material related to this article can be found online at http://doi:10.1016/j.ydbio.2017.08.016.

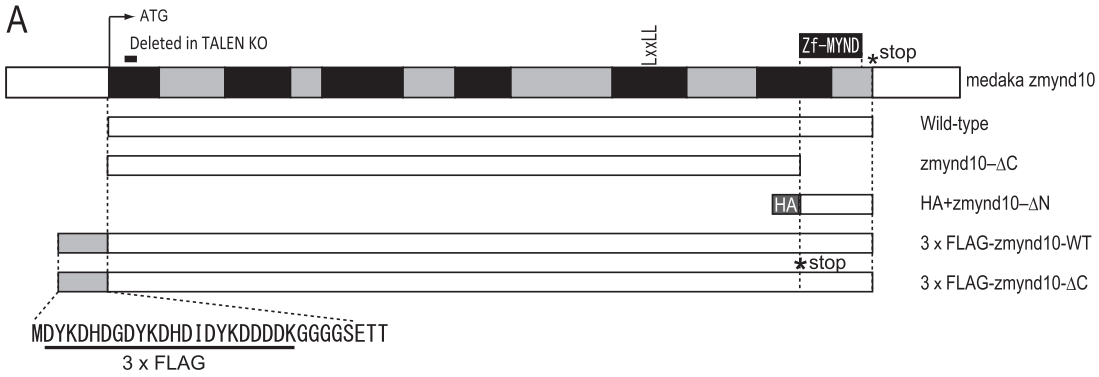

B

Mo-*zmynd10* (μM)		mRNA (ng/μl)	LR-defect		Counted		Total
Mo-TB	Mo-SB	*zmynd10*	#	%	#	%	
200	200	230(medaka zmynd10-ΔC)	16	25.0	64	64.0	100
200	200	590(medaka zmynd10-ΔC)	19	29.7	64	67.4	95
200	200	21(medaka HA+zmynd12-ΔN)	42	56.0	75	62.5	120

C

mRNA	conc. (ng/μl)	Embryos	LR-defect #	LR-defect %	Counted #	Counted %	Total	P value one-sided
3xFLAG-zmynd10-WT	50	Wild-type	0	0.0	32	61.5	52	
3xFLAG-zmynd10-WT	150	Wild-type	5	20.0	25	35.2	71	
3xFLAG-zmynd10-ΔC	50	Wild-type	0	0.0	38	74.5	51	
3xFLAG-zmynd10-ΔC	150	Wild-type	2	9.5	21	60.0	35	
gfp-f	80	zmynd10 (+/-) x (+/-)	10	17.1	70	71.4	98	0.1201
3xFLAG-zmynd10-WT	50	zmynd10 (+/-) x (+/-)	5	4.9	102	56.7	180	0.0102
3xFLAG-zmynd10-ΔC	50	zmynd10 (+/-) x (+/-)	5	4.8	105	81.4	129	0.0083

Total: The total number of injected embryos
Counted: The remaining number of embryos after deduction of those for which laterality could not be determined (dead or abnormal development).
% of Counted: (Counted / Total) x 100
% of LR-defect: (LR-defect / Counted) x 100
gfp-f, membrane bound green fluorescent protein

Fig. 5. mRNA rescue with truncated constructs. (A) Schematic diagram of wild-type (WT) and deletion constructs. (B) Morpholino injection with or without truncated forms of *zmynd10* mRNAs. (C) Injection of 3 × FLAG-tagged WT or ΔC *zmynd10* mRNA partially rescues the LR defect of *zmynd10* KO embryos.

2014). Injected embryos were raised to establish an adult F0 founder population. Genotyping of pooled offspring identified one F0 female founder that transmitted mutations through the germ line. This F0 female was outcrossed to d-rR males and the progeny were genotyped and sequenced. Sequence analysis of one F1 male identified a 12-bp deletion in exon 2, resulting in a 4-aa deletion (Tyr37–Lys40→0; Fig. 1, indicated by white characters). This region contains a single hydrophobic aa, Ile or Leu, that is highly conserved among species (Fig. S3, arrow), while Lys40 is highly conserved among vertebrates (Fig. S1, arrowhead). A missense mutation (Leu39Pro) in this region has also previously been identified in the human *ZMYND10* gene of a PCD patient (Moore et al., 2013). These data suggest that the gene product produced from this mutant allele is likely to have reduced function. The F1 fish were outcrossed to WT and the resulting F2 generation offspring were raised to produce a mutant line for further phenotype analysis.

Phenotype analysis of all the F2 mutant siblings (n = 65) revealed 19.7% curly-tail-down (CTD) embryos and 14.8% LR-defective embryos (Fig. 6A and B). These results suggest that *zmynd10* is a recessive mutation that gives rise to CTD and LR randomization, which are typical phenotypes of motile ciliary mutants. However, it remains unclear whether zmynd10 function is completely abrogated in this mutant. The mutant homozygous fish could not swim and did not survive, probably because of the CTD phenotype. Heterozygous fish showed no obvious phenotype (Fig. 6A). In our previous work, we rescued the CTD phenotypes of *kintoun* and *jaodori* ciliary mutants using WT mRNA injections, which allowed us to observe their phenotypes at later stages of development (Kobayashi et al., 2010; Omran et al., 2008). To analyze the later phenotype of the *zmynd10* mutant, we raised similarly mRNA-rescued embryos and observed scoliosis in the mutant fish (Fig. 6D and H; WT in C and G). These fish also developed progressive renal cysts, with markedly increased tubule diameters (Fig. 6F, K, L; WT in E, I, J). In medaka, the adult kidney is composed of two parts: the head region that occupies most of the kidney, and the tail region that extends to the cloaca (Fedorova et al., 2008). Tubular cysts were observed in both these regions of the kidney (Fig. 6K and L). Because KV cilia motility was lost in the mutant, we assessed sperm motility instead. As expected, sperm motility in the mutant was also completely lost (Video 3, *zmynd10* [−/−]; Video 4, *zmynd10* [+/−]).

4. Discussion

In this study, we showed that zmynd10 is required for cilia morphology integrity and axonemal localization of ODAs. In addition to characteristic PCD phenotypes of LR randomization, CTD and sperm motility defects, *zmynd10* mutant fish developed scoliosis and PKD.

4.1. *zmynd10* and ciliary morphology

As reported in human PCD, zmynd10 is indispensable for proper axonemal localization of dynein arms in medaka KV cilia. In addition to this role, our analyses revealed that zmynd10 is required for formation and/or maintenance of normal cilia, even though their axonemal structure was unaffected. It is possible that the absence of ODAs affects the stiffness of the ciliary membrane, resulting in wavy and swollen cilia. However, our previous results dispute this suggestion: KV cilia in two other ciliary mutants that have defects in ODAs, *ktu* and *joi*, do not

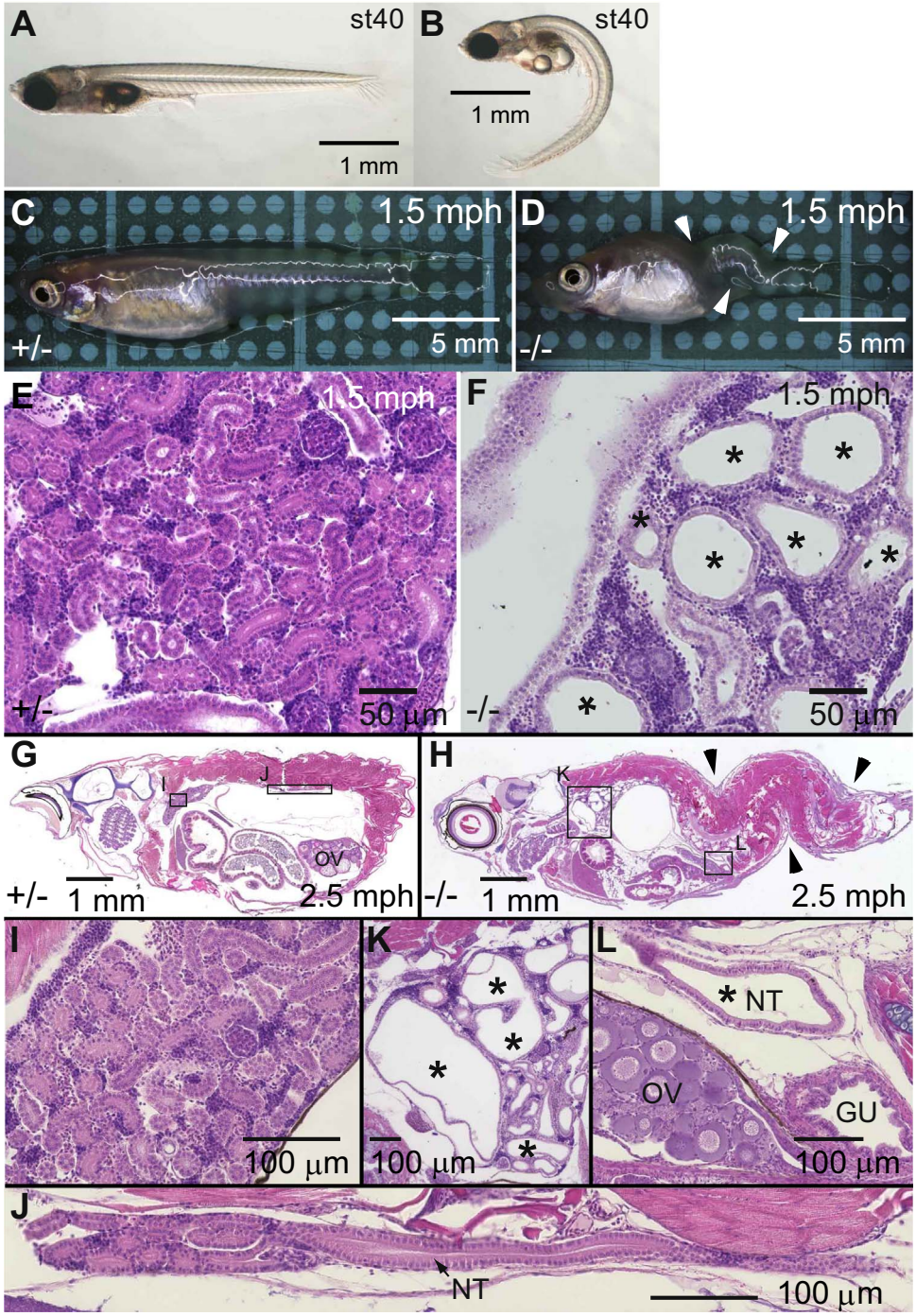

Fig. 6. Medaka zmynd10 mutant phenotypes. Wild-type (A) and *zmynd10* mutant exhibiting the curly-tail-down phenotype (B) at stage 40. The appearances of the heterozygous (C) and *zmynd10* mutant (D) 1.5 months post hatching (mph). (E–J) Histological kidney sections from heterozygous (E, 1.5 mph; G, 2.5 mph) and homozygous *zmynd10* mutants (F, 1.5 mph; H, 2.5 mph). (I–L) Close up images of boxed regions from G and H. Head region of the kidney (I, K). Tail region of the kidney (J, L). OV, ovary; NT, nephric tubule; GU, gut. Asterisks indicate dilated tubules (not all tubules are marked).

have these phenotypes (Kobayashi et al., 2010; Omran et al., 2008). This suggests that zmynd10 may have an additional function, or functions, in ciliary structure besides correct axonemal localization of the dynein arm. Although swollen and wavy cilia is a novel phenotype that was observed in the *zmynd10* mutant, other groups have reported additional zmynd10 functions associated with ciliary morphology including short cilia in hTERT-RPE1 cells (Albee et al., 2013), detachment of the MT doublet complex in fly sperm flagella (Moore et al., 2013), and a reduced number of cilia in epidermal multiciliated cells of *Xenopus laevis* embryos (Zariwala et al., 2013). Together, these studies suggest that zmynd10 is a multi-functional protein that is associated with dynein arm localization and cilia structure formation.

4.2. *Importance of zf-MYND for zmynd10 function*

Our medaka rescue experiment showed that the zmynd10–ΔC truncated protein, which lacks zf-MYND, was still partially functional. Zariwara et al., previously found that the p. Gln366* form of ZMYND10 (Fig. S3, dagger), abrogates ciliary motility and is present in individuals with PCD. This form of ZMYND10 lacks not only zf-MYND, but also its

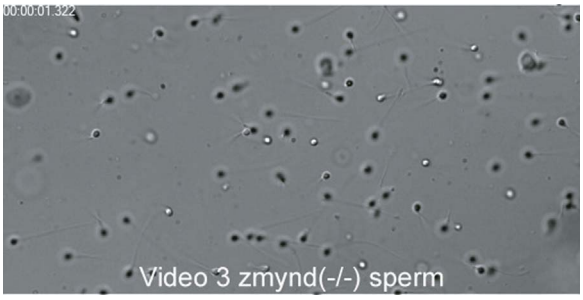

Video 3. Flagellar waveform of *zmynd10*(-/-) mutant sperm showing complete loss of motility. Supplementary material related to this article can be found online at http://doi:10.1016/j.ydbio.2017.08.016.

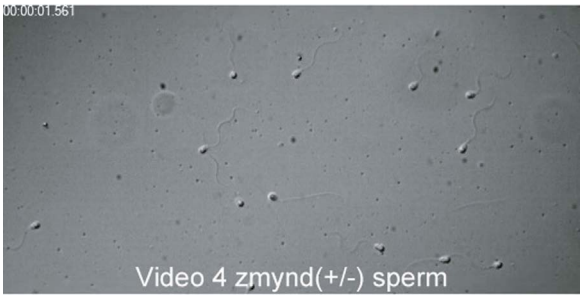

Video 4. Flagellar waveform of wild-type sperm showing bending waves propagating to the tip of the tail. Supplementary material related to this article can be found online at http://doi:10.1016/j.ydbio.2017.08.016.

upstream and downstream sequences. In our experiment, zmynd10–ΔC lacks zf-MYND10 and its downstream sequence, suggesting that the short region between Gln366 and zf-MYND10 is required for complete zmynd10 functionality. It has been reported that ZMYND10 interacts with LRRC6, another causal gene for PCD (Moore et al., 2013; Zariwala et al., 2013), and ZMYND10cannot bind LRRC6 in the absence of zf-MYND (Moore et al., 2013). It had been shown that zf-MYND alone was insufficient for LRRC6 pull-down (Zariwala et al., 2013), but the C-terminal half of ZMYND10, which includes zf-MYND10 domain, interacted with LRRC6 (Moore et al., 2013). Our results further suggest that besides the zf-MYND domain, an additional region is required for complete zmynd10 function.

Albee et al. (2013) identified *zmynd10* as a homolog of a *Chlamydomonas* gene, *Cre08.g358750*, which is upregulated during ciliogenesis. However, unlike *zmynd10*, Cre08.g358750 lacks the region coding for the zf-MYND domain. We performed BLAST searches of the *Chlamydomonas* proteome using human and medaka zmynd10 peptide sequences (JGI phytozome 10.3, *Chlamydomonas reinhardtii* v5.5, http://phytozome.jgi.doe.gov/) and found that Cre08.g358751.t1.1 (an alias of Cre08.g358750) had the highest similarity (human, 8.8E-50; medaka, 8.2E-45). The sequence with the next highest similarity contained the zf-MYND domain; however, similarity was limited to the zf-MYND domain and the E-values were much higher (greater than 1.0E-5, data not shown). Conversely, when we searched the medaka database for homologs of Cre08.g358751.t1.1, *zmynd10* was a top hit. Taken together, BLAST identified human and medaka zmynd10 homologs as reciprocal best hits of Cre08.g358751.t1.1. Moreover, the C-terminal region of Cre08.g358751.t1.1 has intermediate homology scores (NCBI BLAST) to the C-terminal regions of human and medaka zmynd10, even though it lacks the zf-MYND domain. Further analysis will be required to identify any additional functional zmynd10 domains.

4.3. The mechanism of scoliosis in the zmynd10 mutant

The *zmynd10* mutant fish developed scoliosis in the later stages of development. We and another group, Nagao et al. (2010), previously reported this phenotype in another medaka motile ciliary mutant, *joi/mii* (Kobayashi et al., 2010). Taken together, these results suggest that scoliosis is a phenotype of impaired cilia motility in fish. However, another medaka motile ciliary mutant, *ktu*, does not present with scoliosis in adult fish (Omran et al., 2008). The phenotypic differences observed between these ciliary mutants suggest that there is a diversity of motile ciliary components within ciliary organs (discussed further below).

Myxosporean cysts in the fourth ventricle strongly correlate with axial structural abnormalities in aquaculture fish (Maeno and Sorimachi, 1992). These abnormalities may be associated with disruption of normal CSF flow by *Myxosporean* parasites. A similar phenomenon is observed in a rare human disease, Arnold–Chiari malformation (ACM), which is caused by a downward displacement of the cerebellar tonsils through the foramen magnum. In ACM, obstruction of CSF flow also occurs near the fourth ventricle, and scoliosis often supervenes (Milhorat et al., 1999). In human PCD, abnormal body curvatures like scoliosis are not common; however, to our knowledge, five studies have reported PCD with scoliosis (Evander et al., 1983; Baccetti et al., 1993; Tanaka et al., 2007; Yazicioglu et al., 2016; Engesaeth et al., 1993). Moreover, Grimes et al. (2016), recently reported a CSF flow defect that was associated with zebrafish scoliosis. Taken together, these studies suggest that PCD is likely to be a cause of scoliosis. However, whereas the scoliosis phenotype segregates in a recessive Mendelian fashion in fish, it is rare to develop PCD accompanied with scoliosis in humans. It is unclear what might underpin this difference, although it may be due to the different aquatic and terrestrial environments of fish and humans, respectively. Omura et al. (2015) examined trunk vertebrae morphologies in eight urodele species exhibiting different locomotive modes and found that the vertebrae of the more aquatic species have weaker zygapophyseal joints. Because of buoyance, aquatic species do not need to maintain posture; therefore, strong connections between vertebrae are not required. In contrast, human vertebrae need to be more rigid not only because of their terrestrial environment, but also possibly because of bipedalism. These differences may make fish PCD mutants more sensitive to developing scoliosis, and this increased sensitivity may make fish a suitable disease model for evaluating scoliosis risk factors.

4.4. Mechanism of polycystic kidney development in the zmynd10 mutant

Nephric cysts are a characteristic phenotype of medaka and zebrafish mutants that have cilia motility defects (Omran et al., 2008; Sullivan-Brown et al., 2008). In *zmynd10* KO fish, dilatation of the nephric tubule was detected as early as stage 40 (data not shown). Cyst size is likely to continuously increase (compared in Fig. 6F and K), resulting in enlarged kidneys that occupy most of the body cavity. The progression of symptoms through the life of the fish is similar to that observed in human autosomal dominant polycystic kidney disease (AKPKD, (Ferreira et al., 2015)). It has been suggested that cilia motility defects lead to generalized urine retention in the nephron, and that this is the primary cause of cystic dilatations (Kramer-Zucker et al., 2005; Sullivan-Brown et al., 2008). However, renal cysts were also observed near the cloaca (Fig. 6L), suggesting that simple urine retention cannot solely explain the polycystic kidney phenotype of the *zmynd10* mutant. Similar to mammalian systems (Nauli and Zhou, 2004), cilia in fish kidneys may have roles in mechanosensation, and loss of motility, and the reduced urine flow rate may lead to attenuation of mechanical stimulation.

4.5. Diversity of cytoplasmic assembly complexes

The medaka mutant *kintoun* (*ktu*) is a typical motile ciliary mutant (Omran et al., 2008). Whereas KV cilia have complete loss of motility in the *ktu* mutant, sperm retains partial motility. In contrast, the *zmynd10* mutant showed complete loss of motility in both KV cilia and sperm flagella. Both ktu and zmyd10 are reported to be cytoplasmic factors that are required for axonemal dynein arm assembly. However, the phenotypic differences between *ktu* and *zmynd10* mutants suggests that there is diversity in the cytoplasmic assembly complexes of the axonemal dynein arms. In humans, differential distribution of the ODA heavy chains along the axoneme has been reported, with the components of the ODA complexes varying between the respiratory ciliary axoneme and the axoneme of the sperm tail (Fliegauf et al., 2005). Differential requirements of cytoplasmic assembly complexes in different tissues may explain the differences in sperm motility between *ktu* and *zmynd10* mutants.

5. Conclusions

In summary, we have shown that zmynd10 is indispensable for motile ciliary function through its role in both axonemal dynein arm localization and normal ciliary morphology. We propose that region(s) in addition to zf-MYND are required for full zmynd10 activity. *Zmynd10* KO fish that develop scoliosis and PKD may be useful for investigating the pathogenic mechanisms of those diseases.

Acknowledgments

We thank Dr Tatsuya Tsukahara and Prof. Hiroyuki Takeda (The University of Tokyo) for producing the video recordings of KV cilia movement. The hatching enzyme and the d-rR medaka strain used in this research were provided by the medaka NBRP (Ministry of Education, Culture, Sports, Science and Technology, Japan). This research was financially supported by the Narishige Zoological Science Award (2013). We thank Shelley Robison, PhD, from Edanz Group (www.edanzediting.com/ac) for editing a draft of this manuscript.

Appendix A. Supporting information

Supplementary data associated with this article can be found in the online version at http://doi:10.1016/j.ydbio.2017.08.016.

References

Albee, A.J., Kwan, A.L., Lin, H., Granas, D., Stormo, G.D., Dutcher, S.K., 2013. Identification of cilia genes that affect cell-cycle progression using whole-genome transcriptome analysis in Chlamydomonas reinhardtti. Genes Genome Genet. 3 (6), 979–991.
Ansai, S., Sakuma, T., Yamamoto, T., Ariga, H., Uemura, N., Takahashi, R., et al., 2013. Efficient targeted mutagenesis in medaka using custom-designed transcription activator-like effector nucleases. Genetics 193 (3), 739–749.
Ansai, S., Inohaya, K., Yoshiura, Y., Schartl, M., Uemura, N., Takahashi, R., et al., 2014. Design, evaluation, and screening methods for efficient targeted mutagenesis with transcription activator-like effector nucleases in medaka. Dev. Growth Differ. 56 (1), 98–107.
Baccetti, B., Burrini, A.G., Capitani, S., Collodel, G., Moretti, E., Piomboni, P., et al., 1993. Notulae seminologicae. 1. New combinations of Kartagener's syndrome. Andrologia 25 (6), 325–329.
Brummett, A.R., Dumont, J.N., 1978. Kupffer's vesicle in Fundulus heteroclitus: a scanning and transmission electron microscope study. Tissue Cell 10 (1), 11–22.
Engesaeth, V.G., Warner, J.O., Bush, A., 1993. New associations of primary ciliary dyskinesia syndrome. Pediatr. Pulmonol. 16 (1), 9–12.
Essner, J.J., Vogan, K.J., Wagner, M.K., Tabin, C.J., Yost, H.J., Brueckner, M., 2002. Conserved function for embryonic nodal cilia. Nature 418 (6893), 37–38.
Evander, E., Arborelius, M., Jr., Jonson, B., Simonsson, B.G., Svensson, G., 1983. Lung function and bronchial reactivity in six patients with immotile cilia syndrome. Eur. J. Respir. Dis. 127, 137–143.
Fedorova, S., Miyamoto, R., Harada, T., Isogai, S., Hashimoto, H., Ozato, K., et al., 2008. Renal glomerulogenesis in medaka fish, Oryzias latipes. Dev. Dyn. 237 (9), 2342–2352.
Ferreira, F.M., Watanabe, E.H., Onuchic, L.F. Polycystins, 2015. and Molecular Basis of Autosomal Dominant Polycystic Kidney Disease. In: Li, X. (Ed.), Polycystic Kidney Disease. Codon Publications, Brisbane (AU).
Fliegauf, M., Olbrich, H., Horvath, J., Wildhaber, J.H., Zariwala, M.A., Kennedy, M., et al., 2005. Mislocalization of DNAH5 and DNAH9 in respiratory cells from patients with primary ciliary dyskinesia. Am. J. Respir. Crit. Care Med. 171 (12), 1343–1349.
Gawantka, V., Pollet, N., Delius, H., Vingron, M., Pfister, R., Nitsch, R., et al., 1998. Gene expression screening in Xenopus identifies molecular pathways, predicts gene function and provides a global view of embryonic patterning. Mech. Dev. 77 (2), 95–141.
Grimes, D.T., Boswell, C.W., Morante, N.F., Henkelman, R.M., Burdine, R.D., Ciruna, B., 2016. Zebrafish models of idiopathic scoliosis link cerebrospinal fluid flow defects to spine curvature. Science 352 (6291), 1341–1344.
Hoh, R.A., Stowe, T.R., Turk, E., Stearns, T., 2012. Transcriptional program of ciliated epithelial cells reveals new cilium and centrosome components and links to human disease. PLoS One 7 (12), e52166.
Hojo, M., Takashima, S., Kobayashi, D., Sumeragi, A., Shimada, A., Tsukahara, T., et al., 2007. Right-elevated expression of charon is regulated by fluid flow in medaka Kupffer's vesicle. Dev. Growth Differ. 49 (5), 395–405.
Iwamatsu, T., 2004. Stages of normal development in the medaka Oryzias latipes. Mech. Dev. 121 (7–8), 605–618.
Kamura, K., Kobayashi, D., Uehara, Y., Koshida, S., Iijima, N., Kudo, A., et al., 2011. Pkd1l1 complexes with Pkd2 on motile cilia and functions to establish the left-right axis. Development 138, 1121–1129.
Kobayashi, D., Takeda, H., 2012. Ciliary motility: the components and cytoplasmic preassembly mechanisms of the axonemal dyneins. Differentiation 83 (2), S23–S29.
Kobayashi, D., Iijima, N., Hagiwara, H., Kamura, K., Takeda, H., Yokoyama, T., 2010. Characterization of the medaka (Oryzias latipes) primary ciliary dyskinesia mutant, jaodori: redundant and distinct roles of dynein axonemal intermediate chain 2 (dnai2) in motile cilia. Dev. Biol. 347 (1), 62–70.
Kramer-Zucker, A.G., Olale, F., Haycraft, C.J., Yoder, B.K., Schier, A.F., Drummond, I.A., 2005. Cilia-driven fluid flow in the zebrafish pronephros, brain and Kupffer's vesicle is required for normal organogenesis. Development 132 (8), 1907–1921.
Kudoh, T., Tsang, M., Hukriede, N.A., Chen, X., Dedekian, M., Clarke, C.J., et al., 2001. A gene expression screen in zebrafish embryogenesis. Genome Res. 11 (12), 1979–1987.
Kurkowiak, M., Zietkiewicz, E., Witt, M., 2015. Recent advances in primary ciliary dyskinesia genetics. J. Med. Genet. 52 (1), 1–9.
Lerman, M.I., Minna, J.D., 2000. The 630-kb lung cancer homozygous deletion region on human chromosome 3p21.3: identification and evaluation of the resident candidate tumor suppressor genes. The International Lung Cancer Chromosome 3p21.3 Tumor Suppressor Gene Consortium. Cancer Res. 60 (21), 6116–6133.
Loges, N.T., Olbrich, H., Fenske, L., Mussaffi, H., Horvath, J., Fliegauf, M., et al., 2008. DNAI2 mutations cause primary ciliary dyskinesia with defects in the outer dynein arm. Am. J. Hum. Genet. 83 (5), 547–558.
Long, S., Ahmad, N., Rebagliati, M., 2003. The zebrafish nodal-related gene southpaw is required for visceral and diencephalic left-right asymmetry. Development 130 (11), 2303–2316.
Maeno, Y., Sorimachi, M., 1992. Skeletal Abnormalities of Fishes Caused by Parasitism of Myxosporea 111. NOAA Tech Rep NMFS, 113–118.
McClintock, T.S., Glasser, C.E., Bose, S.C., Bergman, D.A., 2008. Tissue expression patterns identify mouse cilia genes. Physiol. Genom. 32 (2), 198–206.
Milhorat, T.H., Chou, M.W., Trinidad, E.M., Kula, R.W., Mandell, M., Wolpert, C., et al., 1999. Chiari I malformation redefined: clinical and radiographic findings for 364 symptomatic patients. Neurosurgery 44 (5), 1005–1017.
Moore, D.J., Onoufriadis, A., Shoemark, A., Simpson, M.A., zur Lage, P.I., de Castro, S.C., et al., 2013. Mutations in ZMYND10, a gene essential for proper axonemal assembly of inner and outer dynein arms in humans and flies, cause primary ciliary dyskinesia. Am. J. Hum. Genet. 93 (2), 346–356.
Nagao, Y., Cheng, J., Kamura, K., Seki, R., Maeda, A., Nihei, D., et al., 2010. Dynein axonemal intermediate chain 2 is required for formation of the left-right body axis and kidney in medaka. Dev. Biol. 347 (1), 53–61.
Nagata, K., Hashimoto, C., Watanabe-Asaka, T., Itoh, K., Yasuda, T., Ohta, K., et al., 2016. In vivo 3D analysis of systemic effects after local heavy-ion beam irradiation in an animal model. Sci. Rep. 6, 28691.
Nauli, S.M., Zhou, J., 2004. Polycystins and mechanosensation in renal and nodal cilia. Bioessays 26 (8), 844–856.
Omran, H., Kobayashi, D., Olbrich, H., Tsukahara, T., Loges, N.T., Hagiwara, H., et al., 2008. Ktu/PF13 is required for cytoplasmic pre-assembly of axonemal dyneins. Nature 456 (7222), 611–616.
Omura, A., Ejima, K.I., Honda, K., Anzai, W., Taguchi, Y., Koyabu, D., et al., 2015. Locomotion pattern and trunk musculoskeletal architecture among Urodela. Acta Zool. 96 (2), 225–235.
Riley, B.B., Zhu, C., Janetopoulos, C., Aufderheide, K.J., 1997. A critical period of ear development controlled by distinct populations of ciliated cells in the zebrafish. Dev. Biol. 191 (2), 191–201.
Ross, A.J., Dailey, L.A., Brighton, L.E., Devlin, R.B., 2007. Transcriptional profiling of mucociliary differentiation in human airway epithelial cells. Am. J. Respir. Cell Mol. Biol. 37 (2), 169–185.
Stubbs, J.L., Oishi, I., Izpisua Belmonte, J.C., Kintner, C., 2008. The forkhead protein Foxj1 specifies node-like cilia in Xenopus and zebrafish embryos. Nat. Genet. 40 (12), 1454–1460.
Sullivan-Brown, J., Schottenfeld, J., Okabe, N., Hostetter, C.L., Serluca, F.C., Thiberge, S.Y., et al., 2008. Zebrafish mutations affecting cilia motility share similar cystic phenotypes and suggest a mechanism of cyst formation that differs from pkd2

morphants. Dev. Biol. 314 (2), 261–275.
Takashima, S., Shimada, A., Kobayashi, D., Yokoi, H., Narita, T., Jindo, T., et al., 2007. Phenotypic analysis of a novel chordin mutant in medaka. Dev. Dyn. 236 (8), 2298–2310.
Tanaka, K., Sutani, A., Uchida, Y., Shimizu, Y., Shimizu, M., Akita, M., 2007. Ciliary ultrastructure in two sisters with Kartagener's syndrome. Med. Mol. Morphol. 40 (1), 34–39.
Wang, W.J., Yeung, H.Y., Chu, W.C., Tang, N.L., Lee, K.M., Qiu, Y., et al., 2011. Top theories for the etiopathogenesis of adolescent idiopathic scoliosis. J. Pediatr. Orthop. 31 (1 Suppl), S14–S27.
Yazicioglu, A., Alici, I.O., Karaoglanoglu, N., Yekeler, E., 2016. Pitfalls and challenges of lung transplant in a patient with kartagener syndrome and scoliosis. Exp. Clin. Transplant..
Yu, X., Ng, C.P., Habacher, H., Roy, S., 2008. Foxj1 transcription factors are master regulators of the motile ciliogenic program. Nat. Genet. 40 (12), 1445–1453.
Zariwala, M.A., Gee, H.Y., Kurkowiak, M., Al-Mutairi, D.A., Leigh, M.W., Hurd, T.W., et al., 2013. ZMYND10 is mutated in primary ciliary dyskinesia and interacts with LRRC6. Am. J. Hum. Genet. 93 (2), 336–345.